Elastoplastic Large Deflection Analysis of Three-Dimensional Steel Frames

Minoru Shugyo[1]

Abstract: A beam element is presented for analysis of the elastoplastic large deflection of three-dimensional (3D) frames that have steel members with semirigid joints. A plastic hinge type formulation was employed, combining the "modified incremental stiffness method," the updated Lagrangian formulation, and numerical integration about the end sections of the element. The end sections of the element are discretized into small areas to estimate the plastic deformations of the element. The elastic and plastic deformations of the element are treated separately. The behavior of a semirigid joint is modeled as the element-end compliance. The method can treat comprehensively the plastic deformations due to torsion and warping. Considering the assumptions of the method, a four-element approximation for a member gives excellent results for a 3D analysis of semirigid and pin-connected steel frames as well as for rigid frames. The adequacy of the method is verified by comparing the results with experimental ones obtained by the writer. Some examples are presented to demonstrate the accuracy and efficiency of the method.

DOI: 10.1061/(ASCE)0733-9445(2003)129:9(1259)

CE Database subject headings: Steel frames; Elastoplasticity; Deflection; Joints; Plastic hinges; Warpage.

Introduction

The ultimate strength and the restoring force characteristics under three-dimensional loading are fundamental and important performance characteristics of a building frame. A large number of analysis methods to examine the performance of beam columns and frames have been proposed (Al-Bermani and Kitipornchai 1990; Kouhia and Tuomala 1993; Liew et al. 1993; Hall and Challa 1995; Izzuddin and Smith 1996; Teh and Clarke 1999). Those methods can be classified into two types: plastic zone and plastic hinge type formulations. One of the merits of the plastic hinge type formulation is the separate treatment of elastic and plastic deformations. This means that a geometrically nonlinear stiffness can be obtained by the principle of stationary potential energy, and the "modified incremental stiffness method" (Stricklin et al. 1971; Washizu 1975) can be used as the numerical procedure. This is because the plastic strain energy is completely dissipated in the zero-length plastic hinges and does not affect the internal force vector of the frame. The modified incremental stiffness method is a self-correcting incremental procedure using the total elastic strain energy of a deflected structure. Hence, the plastic hinge type formulation can provide good accuracy as well as simplicity if the plastic deformation increment vector can be obtained precisely. In addition, the use of the plastic hinge method is suitable for frames with semirigid joints because a semirigid joint can be regarded as a kind of plastic hinge. However, the possibility of use of the plastic hinge method for a problem that contains section warping has not been shown yet.

This paper proposes a new type of accurate beam element for analysis of the elastoplastic large deflection of three-dimensional (3D) frames that have steel members with semirigid joints. The element is of the plastic hinge type. The end sections of the element are discretized into small areas (fibers) to estimate the plastic deformation of the element. The elastic and plastic deformations of the element are treated separately. The elastic nonlinear tangent stiffness matrix of the element is obtained by the principle of stationary potential energy using the updated Lagrangian formulation, while the plastic deformation increments are estimated by the tangent coefficient matrix obtained by numerical integration of the hardening moduli of the fibers about the end sections. Therefore, the method can treat comprehensively the plastic deformations due to torsion and warping.

In contrast, many other investigations concerned with semirigid joints have been conducted (Lui and Chen 1986, 1987; Al-Bermani and Kitipornchai 1992; King and Chen 1994; Shugyo et al. 1996; Shakourzadeh et al. 1999). It seems to the writer that the node zero-length joint element proposed by Shugyo et al. (1996) and by Shakourzadeh et al. (1999) is the most simple and efficient method for modeling the 3D behavior of semirigid joints. In this paper, the tangent stiffness matrix for an element is obtained by introducing the node zero-length joint element as the element-end compliance. The modified incremental stiffness method (Stricklin et al. 1971; Washizu 1975), together with the displacement increment method (Ramm 1982), is employed as the numerical procedure.

Assumptions

The following assumptions are made to form the elastoplastic tangent stiffness matrix of the element:

1. Members have thin-walled closed or open sections;
2. Cross sections remain planar and do not distort in the absence of cross-sectional warping;

[1]Professor, Dept. of Structural Engineering, Nagasaki Univ., Bunkyomachi 1-14, Nagasaki 852-8521, Japan. E-mail: shugyo@st.nagasaki-u.ac.jp

Note. Associate Editor: Billie F. Spencer Jr. Discussion open until February 1, 2004. Separate discussions must be submitted for individual papers. To extend the closing date by one month, a written request must be filed with the ASCE Managing Editor. The manuscript for this paper was submitted for review and possible publication on February 2, 2001; approved on October 31, 2002. This paper is part of the ***Journal of Structural Engineering***, Vol. 129, No. 9, September 1, 2003. ©ASCE, ISSN 0733-9445/2003/9-1259–1267/$18.00.

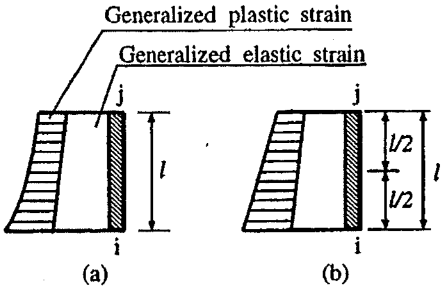

Fig. 1. Assumption of generalized plastic strain distribution in an element

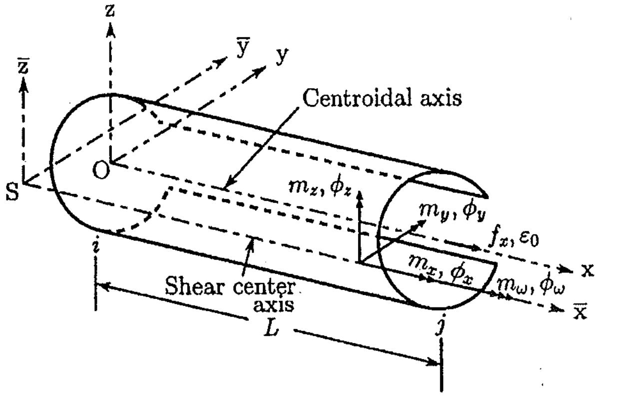

Fig. 2. Element coordinate system and components of generalized stress and strain

3. Transverse shear deformation is negligible;
4. Deflection is large but elastic strain is small;
5. Axial stress and the shear stress due to St. Venant torsion participate in the yielding of the fibers of members with closed sections, while only axial stress participates for the members with open sections;
6. Plastic deformation consists of only four components, which correspond to axial force, biaxial bending moments, and torsional moment (for members with closed sections) or bimoment (for members with open sections);
7. There is no local buckling;
8. Although actual generalized plastic strain in a short element is generally distributed nonlinearly [Fig. 1(a)], the distribution is assumed to be linear with the values at element nodes i and j [Fig. 1(b)];
9. In addition to assumption 8, the concentration of the plastic deformations in the two $l/2$ portions of the element into the plastic hinges of zero length at element nodes i and j is assumed, where l is the length of the element; and
10. In the connection of two or more members (e.g., a beam-column connection) the warping is restrained.

Geometrically Nonlinear Stiffness Matrix

The initial element coordinate systems (x,y,z) and $(\bar{x},\bar{y},\bar{z})$ are shown in Fig. 2 for an element of a general open section. The x axis is perpendicular to the cross section and passes through the centroid O of the end cross section; the y and z axes are the principal axes of the cross section at node i. A parallel set of axes $\bar{x}$, $\bar{y}$, $\bar{z}$ pass through the shear center S of the cross section at node i. The strain-displacement relationship adopted here is

$$
\begin{aligned}
\epsilon_x &= \frac{\partial u}{\partial x} + \frac{1}{2}\left(\frac{\partial v}{\partial x}\right)^2 + \frac{1}{2}\left(\frac{\partial w}{\partial x}\right)^2 \\
\gamma_{xy} &= \frac{\partial v}{\partial x} + \frac{\partial u}{\partial y} \\
\gamma_{xz} &= \frac{\partial w}{\partial x} + \frac{\partial u}{\partial z} \\
\epsilon_y &= \epsilon_z = \gamma_{yz} = 0
\end{aligned}
\tag{1}
$$

where u, v, and w are the displacements of an arbitrary point in the x, y, and z directions, respectively. These values are related to the displacements u_0 of the point on the x axis, v_0, and w_0, and the rotation angle ψ_0 of the point on the $\bar{x}$ axis as

$$
\begin{aligned}
u &= u_0 - y\frac{dv_0}{dx} - z\frac{dw_0}{dx} + \omega_s\frac{d\psi_0}{dx} \\
v &= v_0 - \bar{z}\psi_0 \\
w &= w_0 + \bar{y}\psi_0
\end{aligned}
\tag{2}
$$

where ω_s=normalized warping function about the shear center. Substituting Eq. (2) into Eq. (1) and utilizing the modified incremental stiffness method (Stricklin et al. 1971; Washizu 1975), we obtain the following equation:

$$d\mathbf{Q} + \mathbf{R} = \mathbf{K}^e d\mathbf{q}^e \tag{3}$$

in which $\mathbf{K}^e$ = geometrically nonlinear tangent stiffness matrix; $\mathbf{R}$ = out-of-balance force vector; and $\mathbf{Q}$ and $\mathbf{q}^e$ = nodal force vector and nodal elastic displacement vector of an element, respectively. $\mathbf{Q}$ and $\mathbf{q}^e$ have the following components:

$$
\begin{aligned}
\mathbf{Q} &= [F_{xi} \; F_{yi} \; F_{zi} \; M_{xi} \; M_{yi} \; M_{zi} \; M_{\omega i} \; F_{xj} \; F_{yj} \; F_{zj} \; M_{xj} \; M_{yj} \; M_{zj} \; M_{\omega j}]^T \\
\mathbf{q}^e &= [u_i^e \; v_i^e \; w_i^e \; \theta_{xi}^e \; \theta_{yi}^e \; \theta_{zi}^e \; \theta_{xi}'^e \; u_j^e \; v_j^e \; w_j^e \; \theta_{xj}^e \; \theta_{yj}^e \; \theta_{zj}^e \; \theta_{xj}'^e]^T
\end{aligned}
\tag{4}
$$

where F_{kl} denotes the force in the k direction at node l; M_{kl} denotes the bending or torsional moment about the k axis at node l; and M_{ω_l} denotes the bimoment at node l. Components of $\mathbf{q}^e$ are the corresponding elastic displacements. The rotation matrix for large rotation (Crisfield 1997) was used to determine the successive element coordinate system and the nodal total local displacements. Therefore, some components of the total nodal local displacements that are contained in $\mathbf{K}^e$ at the last known state (the reference configuration) are as follows if the element is in the elastic range: $u_i^e = v_i^e = w_i^e = v_j^e = w_j^e = 0$, and $\theta_{xi}^e = -\theta_{xj}^e$. Cubic functions for v_0, w_0, and ψ_0 and a linear function for u_0 are adopted as displacement fields.

Estimation of Plastic Deformation Increments

In the present formulation, the plastic deformation increment of an element is estimated utilizing a tangent coefficient matrix for the cross section. The tangent coefficient matrix is obtained by numerical integration of the tangent stiffnesses of the fibers that compose the element.

Incremental Stress-Strain Relationship of a Fiber

For a member with a thin-walled closed section, using the von Mises yield condition, associated flow rule, and Ziegler's hardening rule, we can obtain the following equation (Armen et al. 1970; Shugyo et al. 1995) from assumption 5:

$$\begin{Bmatrix} d\sigma \\ d\tau \end{Bmatrix} = \begin{bmatrix} D_{11} & D_{12} \\ D_{21} & D_{22} \end{bmatrix} \begin{Bmatrix} d\epsilon \\ d\gamma \end{Bmatrix} \equiv \mathbf{D} \begin{Bmatrix} d\epsilon \\ d\gamma \end{Bmatrix} \tag{5}$$

where σ = normal stress due to axial force and bending moments; and τ = shear stress due to St. Venant torsion.

For a member with a thin-walled open section, the incremental stress-strain relationship of a fiber is expressed as

$$d\sigma = E_t d\epsilon \tag{6}$$

where σ = normal stress due to axial force, bending moments, and bimoment; and E_t = tangent modulus of the uniaxial stress-strain relationship of a fiber.

Plastic Tangent Coefficient Matrix for a Section

Thin-Walled Closed Section

The components of the generalized stress vector and generalized strain vector are shown in Fig. 2. From assumptions 5 and 6, the components of the generalized stress vector $\mathbf{f}_c$ and generalized strain vector $\boldsymbol{\delta}_c$ for a thin-walled closed section can be written as

$$\mathbf{f}_c = [f_x \quad m_x \quad m_y \quad m_z]^T$$

$$\boldsymbol{\delta}_c = [\epsilon_0 \quad \phi_x \quad \phi_y \quad \phi_z]^T \tag{7}$$

where f_x=axial force; m_x=torsional moment; and m_y and m_z=bending moments. The components of $\boldsymbol{\delta}_c$ are corresponding generalized strains. The increments of the generalized stresses are related to the fiber stress increments by

$$df_x = \int d\sigma\, dA, \quad dm_x = \int d\tau\, h\, dA$$

$$dm_y = \int d\sigma\, z\, dA, \quad dm_z = -\int d\sigma\, y\, dA \tag{8}$$

whereas the fiber strain increments are related to the increments of the generalized strains by

$$d\epsilon = d\epsilon_0 + z\, d\phi_y - y\, d\phi_z$$

$$d\gamma = h\, d\phi_x \tag{9}$$

where h=section constant. If the wall thickness of the tube is constant, $h=r$ for a circular hollow section and $h=ab/(a+b)$ for a rectangular hollow section, where r is the mean radius, a is the mean width, and b is the mean depth of the section (Teh and Clarke 1999). Substituting Eqs. (5) and (9) into Eq. (8), we obtain the incremental generalized stress-generalized strain relationship

$$d\mathbf{f}_c = \begin{bmatrix} \int D_{11} dA & \int D_{12} h\, dA & \int D_{11} z\, dA & -\int D_{11} y\, dA \\ \int D_{21} h\, dA & \int D_{22} h^2 dA & \int D_{21} hz\, dA & -\int D_{21} hy\, dA \\ \int D_{11} z\, dA & \int D_{12} hz\, dA & \int D_{11} z^2 dA & -\int D_{11} yz\, dA \\ -\int D_{11} y\, dA & -\int D_{12} hy\, dA & -\int D_{11} yz\, dA & \int D_{11} y^2 dA \end{bmatrix} d\boldsymbol{\delta}_c \equiv \mathbf{s}\, d\boldsymbol{\delta}_c \tag{10}$$

where $\mathbf{s}$=tangent coefficient matrix. Let $\mathbf{s}^e$ denote the elastic tangent coefficient matrix and let $d\boldsymbol{\delta}_c^e$ and $d\boldsymbol{\delta}_c^p$ denote the elastic and plastic components of $d\boldsymbol{\delta}_c$, respectively; then

$$d\mathbf{f}_c = \mathbf{s}^e d\boldsymbol{\delta}_c^e$$

$$d\boldsymbol{\delta}_c = d\boldsymbol{\delta}_c^e + d\boldsymbol{\delta}_c^p \tag{11}$$

Substituting Eq. (10) into Eq. (11) yields

$$d\boldsymbol{\delta}_c^p = (\mathbf{s}^{-1} - \mathbf{s}^{e^{-1}}) d\mathbf{f}_c \equiv \hat{\mathbf{s}}\, d\mathbf{f}_c \tag{12}$$

where $\hat{\mathbf{s}}$=plastic tangent coefficient matrix. The elastic tangent coefficient matrix $\mathbf{s}^e$ is constant for any state of the section.

Thin-Walled Open Section

We can obtain the plastic tangent coefficient matrix $\hat{\mathbf{s}}$ for an open section in the same way as described above using Eq. (6) instead of Eq. (5) (Chen and Atsuta 1977). The components of the generalized stress vector $\mathbf{f}_o$ and generalized strain vector $\boldsymbol{\delta}_o$ for a thin-walled open section are

$$\mathbf{f}_o = [f_x \quad m_y \quad m_z \quad m_\omega]^T$$

$$\boldsymbol{\delta}_o = [\epsilon_0 \quad \phi_y \quad \phi_z \quad \phi_\omega]^T \tag{13}$$

where m_ω=bimoment; and ϕ_ω=corresponding generalized strain.

For both closed and open sections the components of the tangent coefficient matrix can be obtained by numerical integration. Fig. 3 shows the partitioning of the cross section used in the

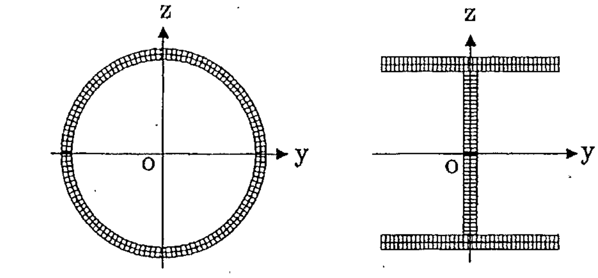

(a) Hollow circular section (b) H-section

Fig. 3. Partitioning of a cross section

analyses described later. The stress and the tangent stiffness in each fiber are obtained as the average values at its centroid. The "tangent stiffness method" (Chen and Atsuta 1977) can be used to determine the matrix s.

Estimation of Plastic Deformation Increments

Now, let us define the plastic deformation increments in the plastic hinges $d\mathbf{q}_i^p$ and $d\mathbf{q}_j^p$ as

$$d\mathbf{q}_i^p=[du_i^p \quad 0 \quad 0 \quad d\theta_{xi}^p \quad d\theta_{yi}^p \quad d\theta_{zi}^p \quad 0]^T$$

$$d\mathbf{q}_j^p=[du_j^p \quad 0 \quad 0 \quad d\theta_{xj}^p \quad d\theta_{yj}^p \quad d\theta_{zj}^p \quad 0]^T \tag{14}$$

for an element with a thin-walled closed section and

$$d\mathbf{q}_i^p=[du_i^p \quad 0 \quad 0 \quad 0 \quad d\theta_{yi}^p \quad d\theta_{zi}^p \quad d\theta_{xi}'^p]^T$$

$$d\mathbf{q}_j^p=[du_j^p \quad 0 \quad 0 \quad 0 \quad d\theta_{yj}^p \quad d\theta_{zj}^p \quad d\theta_{zj}'^p]^T \tag{15}$$

for an element with a thin-walled open section, which are the deformation increments due to the generalized plastic strain increments of an element. These plastic deformation increments can be obtained as described below.

The generalized stresses at the element ends are obtained by the nodal forces at the last known state with their coordinate transformation. (Note that the i-node cross section is the negative plane about the x and $\bar{x}$ axes.) Using these generalized stresses, we can obtain the plastic tangent coefficient matrices $\hat{\mathbf{s}}_i$ and $\hat{\mathbf{s}}_j$ utilizing the procedure explained above. Representing the components of $\hat{\mathbf{s}}_i$ by $(\hat{s}_{kl})_i$, a new square matrix $\mathbf{s}_i^p$ of the seventh order can be obtained as follows:

$$\mathbf{s}_i^p=\begin{bmatrix} (\hat{s}_{11})_i & 0 & 0 & (\hat{s}_{12})_i & (\hat{s}_{13})_i & (\hat{s}_{14})_i & 0 \\ 0 & 0 & 0 & 0 & 0 & 0 & 0 \\ 0 & 0 & 0 & 0 & 0 & 0 & 0 \\ (\hat{s}_{21})_i & 0 & 0 & (\hat{s}_{22})_i & (\hat{s}_{23})_i & (\hat{s}_{24})_i & 0 \\ (\hat{s}_{31})_i & 0 & 0 & (\hat{s}_{32})_i & (\hat{s}_{33})_i & (\hat{s}_{34})_i & 0 \\ (\hat{s}_{41})_i & 0 & 0 & (\hat{s}_{42})_i & (\hat{s}_{43})_i & (\hat{s}_{44})_i & 0 \\ 0 & 0 & 0 & 0 & 0 & 0 & 0 \end{bmatrix} \tag{16}$$

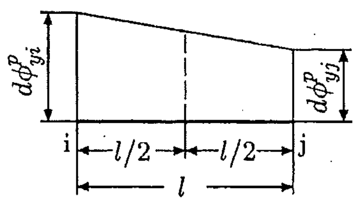

Fig. 4. Assumed plastic curvature distribution in an element

for a closed section element and

$$\mathbf{s}_i^p=\begin{bmatrix} (\hat{s}_{11})_i & 0 & 0 & 0 & (\hat{s}_{12})_i & (\hat{s}_{13})_i & (\hat{s}_{14})_i \\ 0 & 0 & 0 & 0 & 0 & 0 & 0 \\ 0 & 0 & 0 & 0 & 0 & 0 & 0 \\ 0 & 0 & 0 & 0 & 0 & 0 & 0 \\ (\hat{s}_{21})_i & 0 & 0 & 0 & (\hat{s}_{22})_i & (\hat{s}_{23})_i & (\hat{s}_{24})_i \\ (\hat{s}_{31})_i & 0 & 0 & 0 & (\hat{s}_{32})_i & (\hat{s}_{33})_i & (\hat{s}_{34})_i \\ (\hat{s}_{41})_i & 0 & 0 & 0 & (\hat{s}_{42})_i & (\hat{s}_{43})_i & (\hat{s}_{44})_i \end{bmatrix} \tag{17}$$

for an open section element. Another new matrix $\mathbf{s}_j^p$ that corresponds to $\hat{\mathbf{s}}_j$ can be similarly obtained. In the case of uniaxial bending, the plastic curvature increment is distributed as shown in Fig. 4 from assumption 8. Hence the plastic rotation increment at the element end i can be expressed as follows using the trapezoidal rule from assumptions 8 and 9:

$$-d\theta_{yi}^p=\frac{1}{2}\cdot\frac{l}{2}\left\{d\phi_{yi}^p+\frac{1}{2}(d\phi_{yi}^p+d\phi_{yj}^p)\right\}=\frac{l}{2}\cdot\frac{3d\phi_{yi}^p+d\phi_{yj}^p}{4} \tag{18}$$

The plastic deformation increments at the element end i can be obtained by extending Eq. (18), considering that the i-node section is a negative plane and expressed as

$$d\mathbf{q}_i^p=\frac{l}{2}\cdot\frac{3\mathbf{s}_i^p d\mathbf{Q}_i-\mathbf{s}_j^p d\mathbf{Q}_j}{4} \tag{19}$$

Similarly, for the element end j

$$d\mathbf{q}_j^p=\frac{l}{2}\cdot\frac{-\mathbf{s}_i^p d\mathbf{Q}_i+3\mathbf{s}_j^p d\mathbf{Q}_j}{4} \tag{20}$$

Rearranging Eqs. (19) and (20), we obtain

$$\begin{Bmatrix} d\mathbf{q}_i^p \\ d\mathbf{q}_j^p \end{Bmatrix}=\frac{l}{8}\begin{bmatrix} 3\mathbf{s}_i^p & -\mathbf{s}_j^p \\ -\mathbf{s}_i^p & 3\mathbf{s}_j^p \end{bmatrix}\begin{Bmatrix} d\mathbf{Q}_i \\ d\mathbf{Q}_j \end{Bmatrix}\equiv\mathbf{s}^p d\mathbf{Q} \tag{21}$$

Deformation Increments in Semirigid Joints

The matrix $\mathbf{s}^p$ in Eq. (21) is a compliance matrix that relates the nodal plastic deformation increment vector to the nodal force increment vector. Almost the same expression can be written for the deformation increment vector in a semirigid joint at node i if the interaction effects are negligible (Shugyo et al. 1996; Shakourzadeh et al. 1999), as follows:

$$d\mathbf{q}_i^s=\begin{bmatrix} 0 & 0 & 0 & 0 & 0 & 0 & 0 \\ 0 & 0 & 0 & 0 & 0 & 0 & 0 \\ 0 & 0 & 0 & 0 & 0 & 0 & 0 \\ 0 & 0 & 0 & (c_{44})_i & 0 & 0 & 0 \\ 0 & 0 & 0 & 0 & (c_{55})_i & 0 & 0 \\ 0 & 0 & 0 & 0 & 0 & (c_{66})_i & 0 \\ 0 & 0 & 0 & 0 & 0 & 0 & (c_{77})_i \end{bmatrix} d\mathbf{Q}_i\equiv\mathbf{c}_i d\mathbf{Q}_i \tag{22}$$

where $d\mathbf{q}_i^s$ = deformation increment vector in the zero length semirigid element at node i. Similarly, we can obtain the matrix $\mathbf{c}_j$ for node j and hence

$$d\mathbf{q}^s=\mathbf{c}d\mathbf{Q} \tag{23}$$

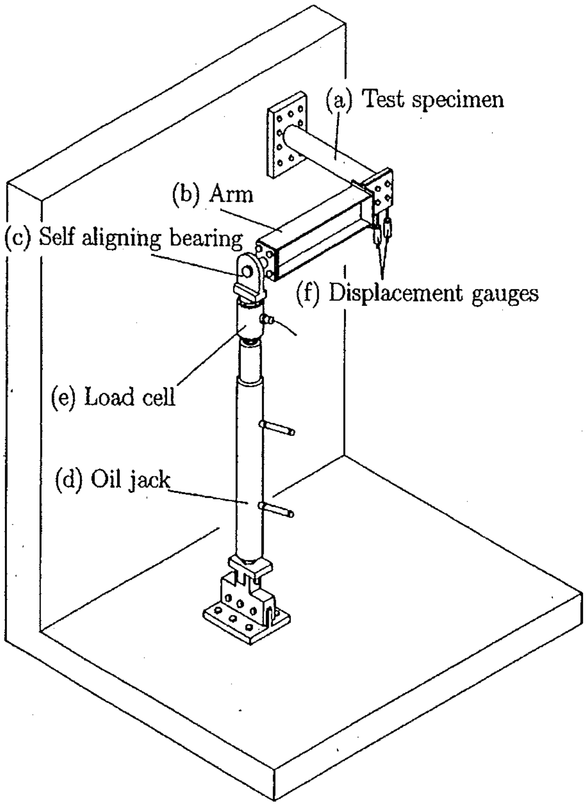

Fig. 5. Test arrangement for cantilever beam

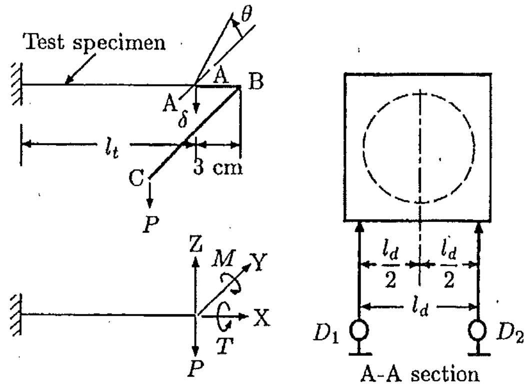

Fig. 6. Scheme of loading and measuring system

If the interaction curve for the semirigid joint is given, the interaction effects may be introduced into the matrix **c** using plastic theory.

Elastoplastic Tangent Stiffness Matrix

Assuming that the total displacement increment $d\mathbf{q}$ is the sum of the elastic displacement increment $d\mathbf{q}^e$, the plastic deformation increment $d\mathbf{q}^p$, and the deformation increment in the zero-length semirigid elements $d\mathbf{q}^s$, we obtain

$$d\mathbf{q}^e = d\mathbf{q} - d\mathbf{q}^p - d\mathbf{q}^s \tag{24}$$

From Eq. (3) the linearized relationship between $d\mathbf{Q}$ and $d\mathbf{q}^e$ is given as $d\mathbf{Q}=\mathbf{K}^e d\mathbf{q}^e$; hence

$$d\mathbf{Q} = \mathbf{K}^e d\mathbf{q} - \mathbf{K}^e(d\mathbf{q}^p + d\mathbf{q}^s) \tag{25}$$

Substituting Eqs. (21) and (23) into Eq. (25), we obtain

$$d\mathbf{Q} = \mathbf{K}^e d\mathbf{q} - \mathbf{K}^e(\mathbf{s}^p + \mathbf{c})d\mathbf{Q} \tag{26}$$

Rearranging Eq. (26) and again introducing the concept of modified incremental stiffness, we can obtain the following equation:

$$d\mathbf{Q} + \mathbf{R} = [\mathbf{I} + \mathbf{K}^e(\mathbf{s}^p + \mathbf{c})]^{-1}\mathbf{K}^e d\mathbf{q} \equiv \mathbf{K}^p d\mathbf{q} \tag{27}$$

where $\mathbf{I}$=unit matrix; $\mathbf{R}$=out-of-balance force vector; and $\mathbf{K}^p$ =elastoplastic tangent stiffness matrix. The numerical analysis can be conducted by Ramm's displacement increment method (Ramm 1982) using Eq. (27). The coordinate transformation matrix of an element is updated and the total nodal local displacements are recomputed by separating the rigid body displacements at each step by using the rotation matrix. $\mathbf{R}$ is obtained from explicit expressions using the elastic total nodal local displacements, which can be obtained by subtracting the sum of the plastic deformation increments and the deformation increments in the semirigid elements from the total nodal local displacements.

The use of the modified incremental stiffness method may cause a significant error if the size of the displacement increment is not appropriate. Therefore, the writer used the following procedure to determine the size of the displacement increment. (1) Examine the magnitude of the generalized strain increments in the last step for all elements and obtain the maximum value. (2) Determine the size of the displacement increment of the next step using the sizes of the displacement increment and maximum generalized strain increment in the last step so that the maximum

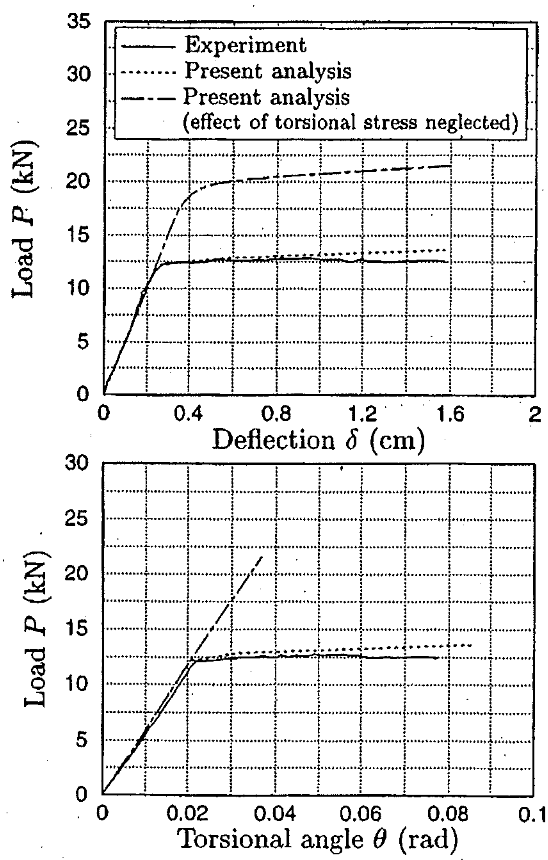

Fig. 7. Load-deflection and load-torsional angle relationships at tip of beam (hollow circular section)

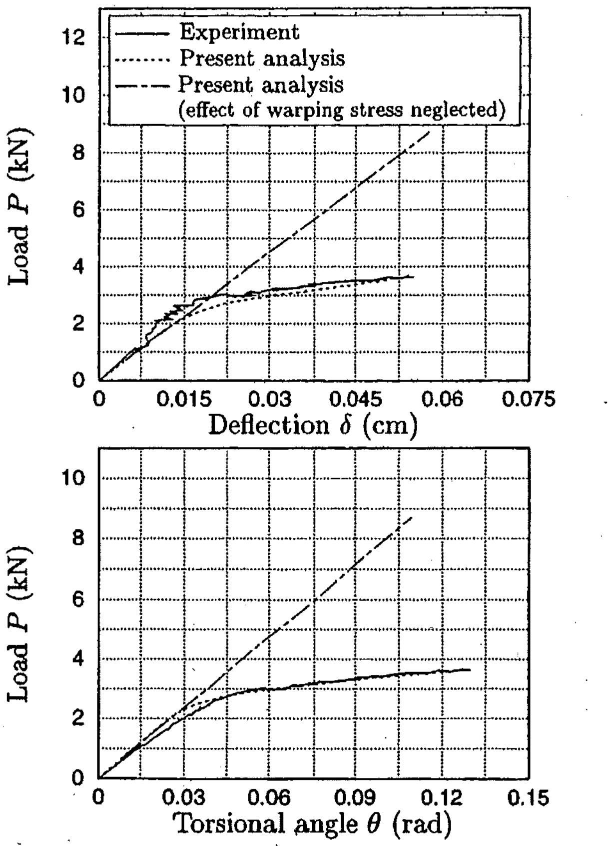

Fig. 8. Load-deflection and load-torsional angle relationships at tip of beam (H section)

value of the generalized strain increment in the next step is less than the prescribed standard value. As the standard value for all the following examples, the writer used a value of 0.01, which is the nondimensionalized value determined by the initial yield value of each element.

Numerical Examples

Cantilever Beams Subjected to Shear Force and Torsional Moment

The adequacy of the present method in determining the bending-torsional behavior of a beam is examined by comparing the results with experimental results of cantilever beams subjected to shear force and torsional moment. Fig. 5 shows the test arrangement. The test specimens were two steel beams, one with a hollow circular section and one with an H section. Both specimens were annealed at 630°C for 1 h. The sizes and mechanical properties of the specimens are as follows: outside diameter of the cross section $D_c = 10.17$ cm, thickness $t_c = 0.41$ cm, length $l_t = 55.30$ cm, Young's modulus $E_c = 207.8$ GPa, yield stress $\sigma_{yc} = 299.9$ MPa for the beam with the hollow circular section; and width of the section $W_h = 10.10$ cm, depth $D_h = 10.00$ cm, flange thickness $t_f = 0.77$ cm, web thickness $t_w = 0.57$ cm, length $l_t = 51.40$ cm, Young's modulus $E_h = 205.8$ GPa, yield stress $\sigma_{yh} = 271.5$ MPa for the beam with the H section.

Fig. 6 shows the scheme of the loading and measuring system. The distance from point B to point C in the figure is 73.0 cm. The load P causes the shear force P, the bending moment M, and the torsional moment T at the tip of the test specimen (A-A section), where $M = 3P$ and $T = 73\cos\theta\, P$. The H beam was set so the weak axis of the cross section was aligned with the direction of the shear force. The warping of both end sections was restrained by end plates 3.0 cm thick. The vertical deflection δ and torsional angle θ can be obtained from the outputs of two displacement gauges δ_1 and δ_2 as follows:

$$\delta = (\delta_1 + \delta_2)/2$$
$$\theta = \tan^{-1}[(\delta_2 - \delta_1)/l_d] \quad (28)$$

In the numerical analyses, the elastic shear moduli $G_c = E_c/2.6$, $G_h = E_h/2.6$ and strain hardening moduli in the elastoplastic range $H_c = E_c/100$, $H_h = E_h/100$ were assumed in addition to the above-mentioned material constants. Considering assumption 8 of the method, the beam was divided into two elements by the node at a point 1/5 of the beam length. The relationships of load versus vertical deflection and load versus torsional angle at the beam tip are shown in Figs. 7 and 8. The dot-dashed lines in the figures are the curves for the cases where the effects of torsional and warping stresses for plastic behavior are neglected. Although some errors are present, the figures show that this method gives an accurate result for a beam member. Since the torsional deformation in the H beam specimen is produced mainly

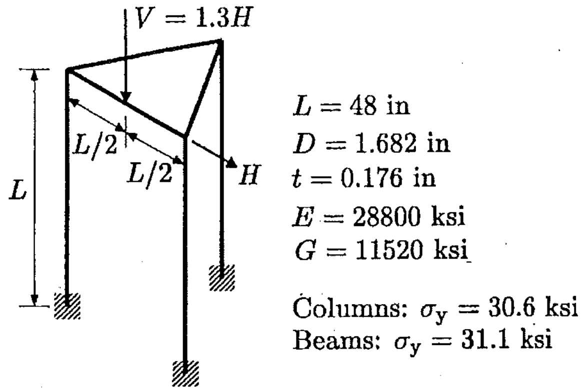

Fig. 9. Harrison's (1964) space frame

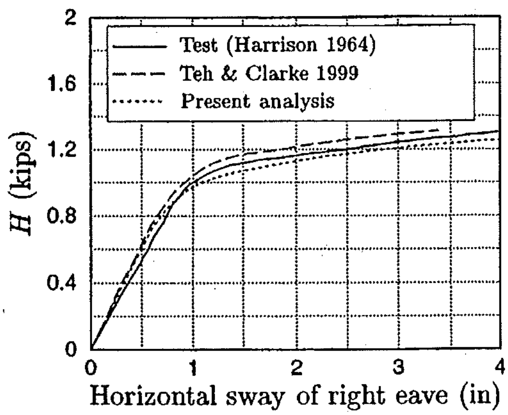

Fig. 10. Load-displacement curves for Harrison's (1964) space frame

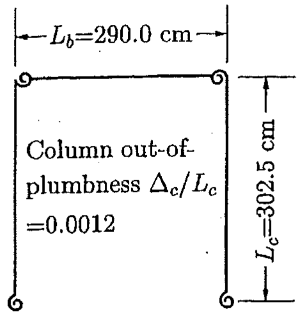

Fig. 11. Semirigid rectangular frame SRF5 (Liew et al. 1997)

by the in-plane bending of the flanges due to section warping, the restoring force for the H-beam specimen increases considerably after the initial yielding.

Three-Dimensional Frame

The adequacy of the present method on the elastoplastic behavior of a 3D frame is examined by using the equilateral triangular space frame tested and analyzed by Harrison (1964) and by Teh and Clarke (1999) (Fig. 9). The properties of the members are given in the figure. All members are steel pipes with hollow circular section. In the present analysis, each member was modeled in the same manner as by Teh and Clarke (1999), that is, each column was modeled with four equal-length elements, while the beams were modeled with two or six equal-length elements considering the loading condition. The strain hardening modulus $H = E/100$ was assumed, whereas Teh and Clarke (1999) assumed $H=0$.

Fig. 10 compares the relationship between the horizontal load and the horizontal sway of the right eave. The result of the present method agrees with the numerical results of Teh and Clarke (1999) in the elastic range; the restoring force in the elastoplastic range is slightly small in comparison with the other two results. As is obvious from assumption 8, the present method overestimates somewhat the plastic deformation of a structure.

Semirigid Rectangular Frame

Liew et al. (1997) carried out a series of tests on a variety of semirigid rectangular frames with H beams and H columns. The test frames can be used for a calibration of analysis method. Fig.

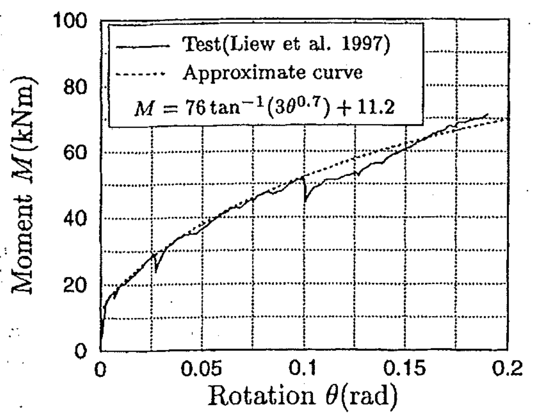

Fig. 12. Moment-rotation curve for beam-column joint (JSRF5)

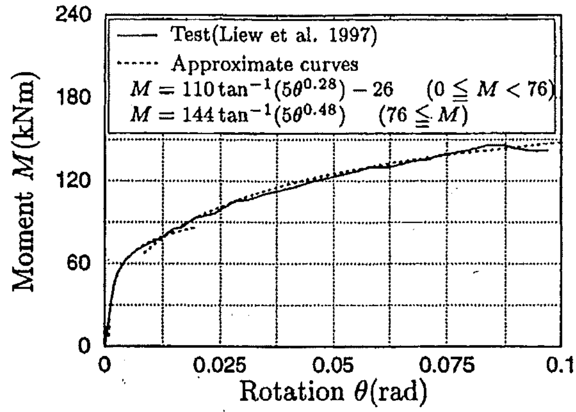

Fig. 13. Moment-rotation curve for column base (CB2)

11 shows the dimensions of the SRF5 frame. The sizes and mechanical properties of the columns and the beam are as follows: depth $D=20.96$ cm, width $B=20.52$ cm, flange thickness $t_f=1.42$ cm, web thickness $t_w=0.93$ cm, yield stress $\sigma_y=336.0$ MPa for the columns, and $D=25.6$ cm, $B=14.64$ cm, $t_f=1.09$ cm, $t_w=0.64$ cm, $\sigma_y=345.0$ MPa for the beam. The moment-rotation relationships for the beam-to-column connection and for the column base obtained by the tests are shown in Figs. 12 and 13. The dotted lines in the figures are the approximate curves used in the present analysis.

In the numerical analyses, the Young's modulus $E=205.8$ GPa, shear modulus $G=E/2.6$, and strain hardening modulus $H=E/100$ were assumed. The beam was divided into three elements of equal length, while the column was divided into four elements by the nodes at points 1/10, 1/2, and 9/10 of the column length.

In Fig. 14, the horizontal load–lateral displacement curve of the SRF5 frame is compared with the analytical result from the present method. The figure shows that the present method has good accuracy and can trace the load-displacement curve after the maximum load.

Hexagonal Frame with Semirigid Joints

Elastic Analysis

The hexagonal frame shown in Fig. 15 has been analyzed by many researchers to check the accuracy of the numerical method

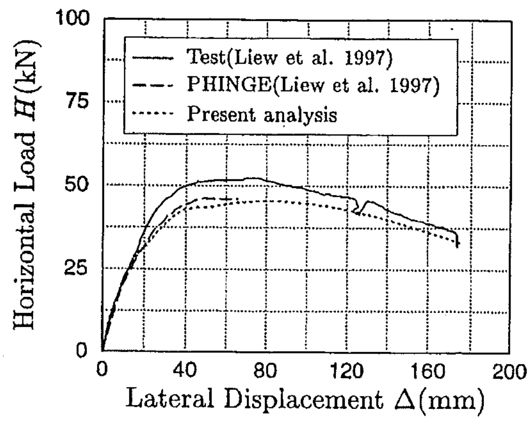

Fig. 14. Comparison of load-displacement curves for SRF5

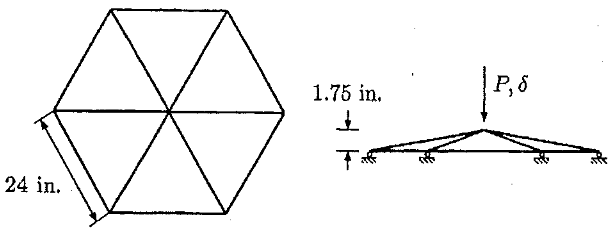

Fig. 15. Hexagonal frame

for analyzing the elastic large deflection behavior of space frames. The properties of the member are as follows: Young's modulus $E=3.032$ GPa (439.8 ksi), shear modulus $G=1.096$ GPa (159.0 ksi), cross-sectional area $A=3.187\ \mathrm{cm}^2$ (0.494 in.^{2}), torsional section constant $J=1.378\ \mathrm{cm}^4$ (0.0331 in.^{4}), and moments of inertia $I_y=I_z=0.832\ \mathrm{cm}^4$ (0.02 in.^{2}). In the present analysis, each member was divided into four elements of equal length.

Fig. 16 compares the load-displacement curve for the rigid frame with those obtained by Chan and Zhou (1994) and by Liew et al. (1999). The curve obtained by the present method agrees closely with other results.

The dotted line and the dot-dashed line are the load-displacement curves for the cases in which both ends of six roof members have semirigid joints and pin joints, respectively. The compliances of the semirigid joints were assumed as 0 for axial force, shear force, and torsional moment, and $L/(2EI_y)$, $L/(2EI_z)$ for bending moments, where L is the member length. For the pin joints, the same assumptions were employed except that $L/(10^{-8}EI_y)$ and $L/(10^{-8}EI_z)$ were used as the compliance for bending moments. The dot-dashed line, which passes through the points (1.75,0) and (3.5,0), shows the adequacy of the method for the analysis of a pin-connected frame.

Elastoplastic Analysis

The results of elastoplastic analyses of the same hexagonal frame with member properties different from the above example are given in Fig. 17. The member was assumed to be a steel pipe with a circular section having cross-sectional area $A=3.187\ \mathrm{cm}^2$. The member properties are as follows: diameter $D=4.674$ cm, thickness $t=0.228$ cm, Young's modulus $E=210.0$ GPa, shear modulus $G=80.77$ GPa, yield stress $\sigma_y=300.0$ MPa, and strain hardening modulus $H=E/100$. Each member was modeled with four equal-length elements. The dotted line and the dot-dashed line in the figure indicate the results for the semirigid and the pin-connected frames. The pin-connected frame did not yield. The result for the rigid frame shows that the load after the frame yielded does not vary acutely.

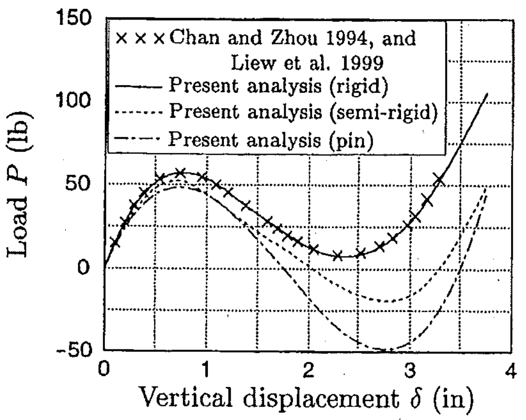

Fig. 16. Load–vertical displacement curves of hexagonal frame

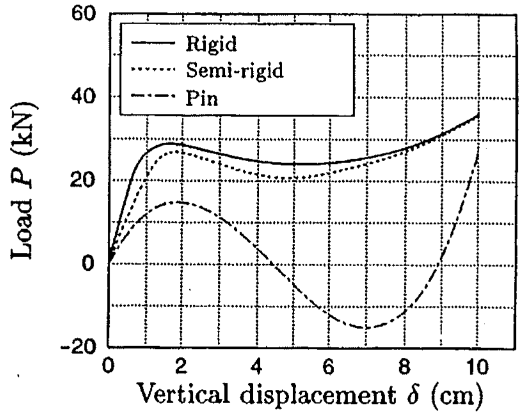

Fig. 17. Load–vertical displacement curves of steel pipe hexagonal frame

Conclusion

An advanced plastic hinge method for accurate analysis of elastoplastic large deflection of three-dimensional steel frames with semirigid joints was presented. The effect of shear stress due to St. Venant torsion on the plastic behavior of a member with a closed section is considered using the von Mises yield criterion, the associated flow rule, and Ziegler's hardening rule. The method can be used for the analyses of frames that have open-section members, which cause section warping. It was shown that the use of the modified incremental stiffness method (Stricklin et al. 1971; Washizu 1975) and the updated Lagrangian formulation, together with a precise estimation of the plastic deformation of an element, gives an accurate result for the 3D analysis of steel frames. The method does not require a database of the yield surfaces of cross sections and can be introduced in an existing finite-element method code. The adequacy of the method was verified by comparing the results with the writer's experimental results. The accuracy and efficiency of the method were examined through the use of several examples. The results of those examinations demonstrated that an approximation of four elements for a member considering the method's assumptions gives excellent results for the 3D analysis of semirigid and pin-connected frames as well as for rigid frames.

References

Al-Bermani, F. G. A., and Kitipornchai, S. (1990). "Elasto-plastic large deformation analysis of thin-walled structures." *Eng. Struct.*, 12, 28–36.

Al-Bermani, F. G. A., and Kitipornchai, S. (1992). "Elastoplastic nonlinear analysis of flexibly jointed space frames." *J. Struct. Eng.*, 118(1), 108–127.

Armen, H., Isakson, G., and Pifko, A. (1970). "Discrete element method for the plastic analysis of structures subjected to cyclic loading." *Int. J. Numer. Methods Eng.*, 2, 189–206.

Chan, S. L., and Zhou, Z. H. (1994). "Pointwise equilibrating polynomial element for nonlinear analysis of frames." *J. Struct. Eng.*, 120(6), 1703–1717.

Chen, W. F., and Atsuta, T. (1977). "Behavior of beam-column segments." *Theory of beam-columns*, Vol. 2, McGraw-Hill, New York, 270–316.

Crisfield, M. A. (1997). *Non-linear finite element analysis of solids and structures, Vol. 2, advanced topics*, Wiley, New York.

Hall, J. F., and Challa, V. R. M. (1995). "Beam-column modeling." *J. Eng. Mech.*, 121(12), 1284–1291.

Harrison, H. B. (1964). "The application of the principles of plastic analysis to three-dimensional steel structures." PhD thesis, Dept. of Civil Engineering, Univ. of Sydney, Australia.

Izzuddin, B. A., and Lloyd Smith, D. (1996). "Large-displacement analysis of elastoplastic thin-walled frames. I: Formulation and implementation." *J. Struct. Eng.*, 122(8), 905–914.

King, W. S., and Chen, W. F. (1994). "Practical second-order inelastic analysis of semirigid frames." *J. Struct. Eng.*, 120(7), 2156–2175.

Kouhia, R., and Tuomala, M. (1993). "Static and dynamic analysis of space frames using simple Timoshenko type elements." *Int. J. Numer. Methods Eng.*, 36, 1189–1221.

Liew, J. Y. R., Chen, H., and Shanmugam, N. E. (1997). "Testing of semi-rigid unbraced frames for calibration of second-order inelastic analysis." *J. Constr. Steel Res.*, 41(2/3), 159–195.

Liew, J. Y. R., Chen, H., and Shanmugam, N. E. (1999). "Stability functions for second-order inelastic analysis of space frames." *Light-Weight Steel and Aluminium Structures, Proc., 4th Int. Conf. on Steel and Aluminium Structures*, Elsevier, Amsterdam, 19–26.

Liew, J. Y. R., White, D. W., and Chen, W. F. (1993). "Second-order refined plastic-hinge analysis for frame design: Part I." *J. Struct. Eng.*, 119(11), 3196–3216.

Lui, E. M., and Chen, W. F. (1986). "Analysis and behaviour of flexibly-jointed frames." *Eng. Struct.*, 8(2), 107–118.

Lui, E. M., and Chen, W. F. (1987). "Steel frame analysis with flexible joints." *J. Constr. Steel Res.*, 8, 161–202.

Ramm, E. (1982). "The Riks/Wempner approach—An extension of the displacement control method in nonlinear analysis." *Recent advances in nonlinear computational mechanics*, Pineridge, Swansee, U.K., 63–86.

Shakourzadeh, H., Guo, Y. Q., and Batoz, J. L. (1999). "Modeling of connection in the analyses of thin-walled space frames." *Comput. Struct.*, 71, 423–433.

Shugyo, M., Li, J. P., and Oka, N. (1995). "Inelastic stability of linearly tapered box columns under biaxial bending and torsion." *Rep. Faculty Eng., Nagasaki Univ.*, 25(45), 143–149.

Shugyo, M., Oka, N., and Li, J. P. (1996). "Inelastic nonlinear analysis of steel space frames with flexible joints." *J. Struct. Constr. Eng.*, 480, 89–94 (in Japanese).

Stricklin, J. A., Haisler, W. E., and von Riesemann, W. A. (1971). "Geometrically nonlinear structural analysis by direct stiffness method." *J. Struct. Div., ASCE*, 97(9), 2299–2314.

Teh, L. H., and Clarke, M. J. (1999). "Plastic-zone analysis of 3D steel frames using beam elements." *J. Struct. Eng.*, 125(11), 1328–1337.

Washizu, K. (1975). "A formulation for the compatible model and the modified incremental stiffness method." *Variational methods in elasticity and plasticity*, 2nd Ed., Pergamon, Oxford, 381–383.